Atmospheric
Measurement
Techniques

Open Access

Evaluation of a new JMA aircraft flask sampling system and laboratory trace gas analysis system

K. Tsuboi[1], H. Matsueda[1], Y. Sawa[1], Y. Niwa[1], M. Nakamura[2], D. Kuboike[2], K. Saito[2], H. Ohmori[2], S. Iwatsubo[2], H. Nishi[2], Y. Hanamiya[2], K. Tsuji[2], and Y. Baba[2]

[1]Geochemical Research Department, Meteorological Research Institute, Tsukuba, Japan
[2]Japan Meteorological Agency, Tokyo, Japan

Correspondence to: K. Tsuboi (ktsuboi@mri-jma.go.jp)

Abstract. We established and evaluated a flask air sampling system on a cargo C-130H aircraft, as well as a trace gas measurement system for the flask samples, as part of a new operational monitoring program of the Japan Meteorological Agency (JMA). Air samples were collected during each flight, between Kanagawa Prefecture (near Tokyo) and Minamitorishima (an island located nearly 2000 km southeast of Tokyo), from the air-conditioning system on the aircraft. Prior to the operational employment of the sampling system, a quality assurance test of the sampled air was made by specially coordinated flights at a low altitude of 1000 ft over Minamitorishima and comparing the flask values with those obtained at the surface. Based on our storage tests, the flask samples remained nearly stable until analyses. The trace gas measurement system has, in addition to the nondispersive infrared (NDIR) and vacuum ultraviolet resonance fluorescence (VURF) analyzers, two laser-based analyzers using wavelength-scanned cavity ring-down spectroscopy (WS-CRDS) and off-axis integrated cavity output spectroscopy (ICOS). Laboratory tests of the laser-based analyzers for measuring flask samples indicated relatively high reproducibility with overall precisions of less than ± 0.06 ppm for CO_2, ± 0.68 ppb for CH_4, ± 0.36 ppb for CO, and ± 0.03 ppb for N_2O. Flask air sample measurements, conducted concurrently on different analyzers were compared. These comparisons showed a negligible bias in the averaged measurements between the laser-based measurement techniques and the other methods currently in use. We also estimated that there are no significant isotope effects for CH_4, CO and N_2O using standard gases with industrial isotopic compositions to calibrate the laser-based analyzers, but CO_2 was found to possess isotope effects larger than its analytical precision.

1 Introduction

East Asia is one of the more prominent source areas of anthropogenic trace gases, and their emissions have been rapidly increasing due to the recent economic growth in Asian countries (Akimoto, 2003). For example, growth of carbon dioxide (CO_2) emissions from fossil-fuel burning and industrial processes has been accelerating in East Asia, particularly in China (Gregg et al., 2008). Carbon monoxide (CO) and other gaseous pollutants emitted from East Asia affect not only the regional environment over the western North Pacific (e.g., Sawa et al., 2007; Wada et al., 2011) but also the air quality over the North American continent as a result of the transpacific transport (e.g., Liang et al., 2004). Agricultural activities in Asian regions are also important as major sources in the global budgets of methane (CH_4) (Bergamaschi et al., 2009) and nitrous oxide (N_2O) (Huang et al., 2008). Current attempts to infer trace gas emissions in East Asia by various top–down inverse methods are limited by the sparseness of the available observation data. In particular, aircraft measurements above the planetary boundary layer are useful in constraining and reducing larger uncertainties of regional flux estimates by inversion calculations (e.g., Stephens et al., 2007; Niwa et al., 2012). Thus, maintaining and expanding multispecies observations of atmospheric trace gases over the western North Pacific is necessary to evaluate rapid changes in anthropogenic emissions and their influences from East Asia.

In the western North Pacific region, long-term monitoring of CO_2 and other trace gases such as CH_4 and CO in the boundary layer has been carried out at several ground-based stations (Tohjima et al., 2002; Wada et al., 2011) and on cruise ships (Yashiro et al., 2009; Terao et al., 2011).

Intensive aircraft measurement campaigns have also been carried out to examine the chemical composition of Asian continental outflows (e.g., Jacob et al., 2003; Machida et al., 2003; Sawa et al., 2004). In addition to these snapshot measurements, more aircraft observational data have been provided by measurements in the free troposphere over the western North Pacific from commercial airliner projects such as CONTRAIL (Comprehensive Observation Network for Trace gases by AIrLiner) (Machida et al., 2008; Sawa et al., 2012), CARIBIC (Civil Aircraft for the Regular Investigation of the atmosphere Based on an Instrument Container) (Brenninkmeijer et al., 2007: Schuck et al., 2009), and MOZIC/IAGOS (Measurements of Ozone and Water Vapour by Airbus In-Service Aircraft/In-service Aircraft for a Global Observing System) (e.g., Marenco et al., 1998; IAGOS project, http://www.iagos.org/IAGOS). These observations have mainly focused on the upper troposphere, thus providing very limited aircraft measurements in the middle troposphere over the western North Pacific. Model simulations showed that export of anthropogenic gases from the Asian continent to the western Pacific through the middle troposphere above the planetary boundary layer is particularly important for the transpacific transport (e.g., Liang et al., 2004; Sawa et al., 2007). Thus, more systematic and long-term measurements in the middle troposphere by using regular aircraft observations are still needed to better understand the widespread dispersion of trace gases emitted from Asian sources.

In 2011, the Japan Meteorological Agency (JMA) started a new aircraft observation of trace gases as one of the operational atmospheric monitoring programs over the western North Pacific. The JMA aircraft observation is made by using a cargo aircraft C-130H of the Japan Ministry of Defense (MOD) to collect flask air samples during a regular flight between the mainland of Japan and Minamitorishima once a month. The C-130H aircraft would provide a unique opportunity for a regular observation of atmospheric trace gases in the middle troposphere because of the aircraft's cruising altitude of about 6 km. However, we faced several logistical issues using the military aircraft, such as lack of available electric power and limited space for our instruments, eliminating any possibility of setting up and operating an automated air sampling system (e.g., Machida et al., 2008; Karion et al., 2013). Thus, sampling is performed manually. In collaboration with the Meteorological Research Institute (MRI), the JMA established a flask air sampling method and validated its reliability through laboratory experiments and preliminary test flights. In this paper, we describe the sampling method employed on the C-130H aircraft, and report results of its evaluation tests.

To analyze the C130H aircraft samples, a trace gas measurement system was also developed to measure mole fractions of CO_2, CH_4, CO, and N_2O. We present this measurement system and its performance. Our trace gas measurement system utilizes two laser-based instruments, because

they have several key advantages such as high precision, improved stability, low maintenance, and easier operation, compared with various conventional gas chromatograph (GC) methods. These advantages of the laser-based instruments are suitable for the long-term operational monitoring at JMA, although the higher initial cost compared with nondispersive infrared (NDIR) analyzers or GC techniques is disadvantageous (e.g., Stephens et al., 2011). The laser-based instruments have been field tested and are available for in situ continuous measurements at ground-based stations and aircraft observations (e.g., Chen et al., 2010; Winderlich et al., 2010; WMO, 2011; Richardson et al., 2012; Zellweger et al., 2012; Karion et al., 2013), but their applications for measuring discrete atmospheric samples were limited except for the analysis of the AirCore tubing sample (Karion et al., 2010). We report on the trace gas measurement system using the laser-based instruments that went into our flask sample analysis. This measurement system was tested to evaluate their performances from the point of view of analytical precisions, linearities and measurement biases, in comparison with the other more common methods such as NDIR and GC techniques.

2 Sampling and analysis methods

2.1 Sampling flight

The MOD operates a routine supply flight once a month using a cargo aircraft C-130H from Atsugi base (35°27′ N, 139°27′ E) in Kanagawa Prefecture near Tokyo to a small coral island of Minamitorishima (MNM) (24°17′ N, 153°59′ E), about 2000 km southeast of Tokyo. In cooperation with the Japan Marine Self-Defense Force of the MOD, these flights enable us to regularly collect air samples over the western North Pacific region.

From July to December in 2010, preliminary observation flights using the C-130H aircraft were made to test the manual air sampling procedure on board the aircraft. In particular, specially coordinated flights at a low altitude of 1000 ft during the climb or descent over MNM were carried out in order to evaluate the quality of the mole fraction measurements of the sampled air from the aircraft, by comparing them with the ground-based measurements obtained at the MNM station. Since February 2011, operational observations have been carried out during southbound flights to MNM, which takes about 4 h at a cruising altitude of about 6 km.

2.2 Flask air sampling

Flask air sampling for the C-130H flight is manually operated by two JMA personnel on board the aircraft. Therefore, a diaphragm pump (KNF Neuberger GmbH, Freiburg im Breisgau, Germany, model N022) is modified to be operated by hand, without the electric power supply. Air samples are collected from the air-conditioning system in the

C-130H aircraft, similar to the procedure employed for the Boeing 747 aircraft observation (Matsueda and Inoue, 1996; Machida et al., 2008). Fresh air outside the aircraft is compressed by an engine and fed into the air-conditioning ducts by passing it through a pneumatic system and air cycle packs. A Teflon tube with a diameter of 1/4 in. for the air sampling intake is inserted into the air-conditioning bowing nozzle upstream of the recirculation fan so that the sample air is not contaminated with the cabin air. Because the air-intake nozzle is located near the cockpit, the Teflon tube (7 m long) is laid along the ceiling and extended toward the cabin, where the pump is installed in front of a passenger seat. A stainless-steel filter (60 μm mesh size) is connected to the air sample tube to remove coarse dust from the air-conditioning duct. In front of the pump, a dryer tube (3/4 inch in diameter, 35 cm in length) packed with CO_2-saturated magnesium perchlorate is used to reduce the water vapor in the sample air. The water vapor was not completely removed because of the short residence time of the air sample in the dryer tube, but conversely, the CO_2 absorption/desorption problem was avoided. The sample air passing through the dryer tube is collected into a sample flask by pressurizing it to about 0.4 MPa by means of the diaphragm pump for 1 min after sufficiently flushing the flask at a flow rate of 6–8 L min^{-1} for more than 5 min. The corresponding distance traveled by the aircraft during each 1 min filling was estimated to be about 10 km.

We prepared new cylindrical flasks, each with an internal volume of about 1.7 L (300 mm long, 100 mm, inner diameter), which are made of titanium with a thickness of 1.2 mm to reduce the total weight. The internal surface of the flask is smoothed by electrochemical polishing, and is coated with amorphous silicon with a thickness of less than 1 μm (Smith et al., 2006) to minimize the drift of trace gas mole fractions in the sampled air during storage. This was done to reduce or eliminate the possibility of a gradual increase of CO mole fraction in metal cylinders and flasks (e.g., Novelli et al., 2003; Matsueda et al., 1998). At both ends of each flask, stainless-steel bellows valves (SS-4H, Swagelok) are attached. Furthermore, quick connectors (Swagelok QC series) are adopted to easily connect the sample inlet and vent tubes in the aircraft. Each flask was preconditioned by heating it at 120 °C under a vacuum condition (1×10^{-6} Torr) for 12 h. It has been shown by Murayama et al. (2003) that such treatment is effective in minimizing the CO_2 drift in flask samples. A total of 24 flasks used for each flight are distributed into 4 aluminium packages, so that they can be easily placed on or removed from the aircraft. We collect 20 flask samples during the level flight, as well as 4 samples during the descent portion of the flight over MNM. Sampling locations are determined based on latitude, longitude and altitude from the flight navigation data of the aircraft.

2.3 Trace gas measurement system

We developed a trace gas measurement system to analyze mole fractions of CO_2, CH_4, CO and N_2O in flask air samples collected from the C-130H aircraft flights. This measurement system installed at JMA in Tokyo is comprised of spectroscopic analyzers that include laser-based instruments of a wavelength-scanned cavity ring-down spectroscopy (WS-CRDS) analyzer (Picarro, Inc., CA, USA, model G2301) for CO_2 and CH_4 (Crosson, 2008), and an off-axis integrated cavity output spectroscopy (ICOS) analyzer (Los Gatos Research, Inc., CA, USA, model DLT100) for N_2O and CO (Baer et al., 2002). In addition, two conventional spectroscopic analyzers, one in an NDIR (LI-COR Biosciences, Inc., NE, USA, model LI-7000) for CO_2 and another one in a vacuum ultraviolet resonance fluorescence (VURF) (Aero-Laser GmbH, Garmisch-Partenkirchen, Germany, model AL5002-AIR) for CO (Gerbig et al., 1999), are also combined. This enables us to compare the CO_2 and CO measurements between the conventional and laser-based methods, allowing us to ensure the analytical precision by cross-checking between the two different analyzers for all sample measurements, as well as to reduce any loss of measurements due to one analyzer malfunctioning.

Figure 1 shows a schematic diagram of the trace gas measurement system. The system is designed to automatically measure trace gas mole fractions of 6 flask samples by using a custom-made control board connected to a personal computer (PC) with a custom-made operation software. Sample flasks are connected using VCO (Swagelok Company, Ohio, USA) attachments at the main airflow line. For mole fraction calibration of the sample measurements, multicomponent working standard gases are introduced by using a multiposition rotary valve of ten ports (Valco Instruments Co. Inc., TX, USA, model A44UWE). Before the introduction of the standard gas, a standard gas vent line is opened to exhaust any remaining gas in the pressure regulator attached to the standard gas cylinder. The sample air and standard gas are passed through the cold-trap unit with two Stirling coolers (Twinbird Co., Niigata, Japan, model SC-UE15R), one at −20 °C and another one at −60 °C, to effectively remove the water vapor. These two cold-trap units are installed in parallel to use them alternatively when one sample flow stops due to trapped ice in one of the Stirling coolers. The temperature of the dried sample is then raised to a room temperature by passing through a heating unit to bring the sample air temperature close to the analyzer's cell temperature.

The flow of the dried air sample from the cold-trap unit is then divided and channeled into the four analyzers by switching 2-way valves (Valco Instruments Co. Inc., TX, USA, model A4VL4MWE2) in front of each analyzer. The flow rates into the analyzer cells are kept constant by mass flow controllers (HORIBA STEC, Co., Ltd., Kyoto, Japan, model SEC-E440J) at 40 mL min^{-1} for the VURF and WS-CRDS, 50 mL min^{-1} for the ICOS, and 120 mL min^{-1} for the NDIR.
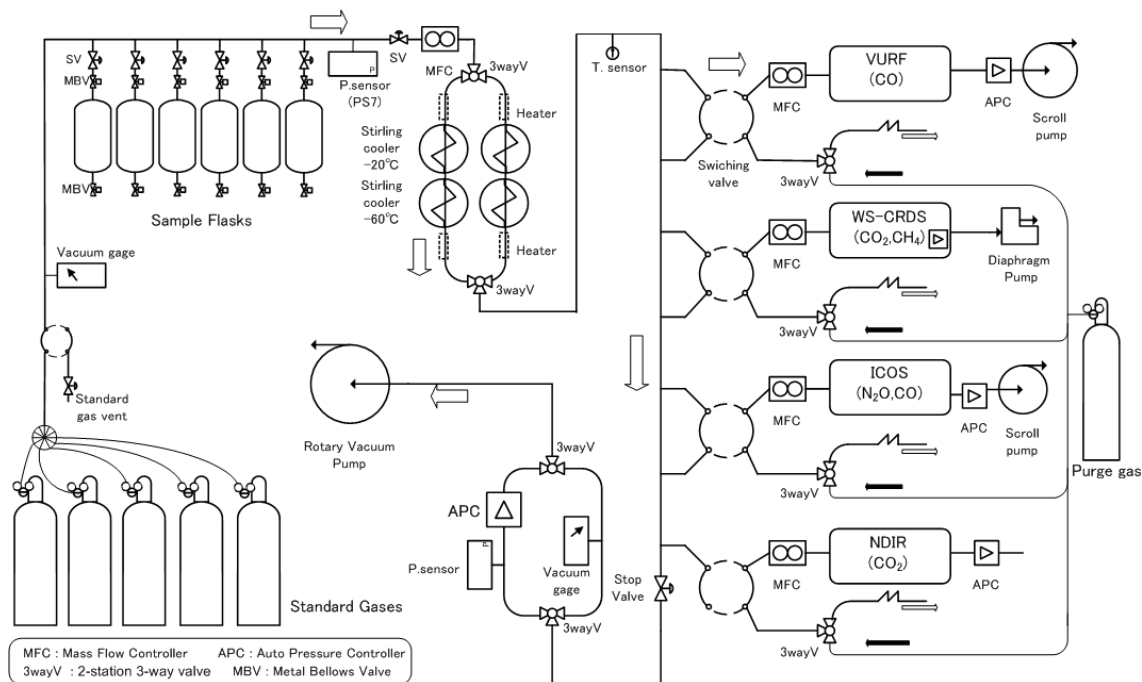
Fig. 1. Schematic diagram of the trace gas measurement system for flask air samples at JMA. Details of the air flow and measuring procedure are described in the text.

Some of these flow rates are low, but they are chosen not only to conserve air samples, but also to synchronize the stabilizing time of all the analyzer responses in order to collect the measured data at the same time. The sample pressures in the analyzer cells are precisely maintained at 0.75 kPa for the VURF, 18.7 kPa for the WS-CRDS, 86 kPa for the ICOS, and 105 kPa for the NDIR by using pressure controllers. The cell pressure for the WS-CRDS analyzer is controlled by its equipped default controller, while custom-made pressure controllers using a piezo valve (HORIBA STEC, Co., Ltd., Kyoto, Japan, model PV-1000/2000 series), instead of their default controllers, are used for the other three analyzers. This configuration reduces the instabilities of the pressure controls due to the lower flow rate. The sample flow into each analyzer is maintained for about 10 min to ensure stabilization of the analyzer responses. After 7 min of the sample flow, the output signals of all analyzers are collected for the last 3 min and their averages are used to calculate the mole fractions.

When we introduce the next flask air sample, the airflow line in front of the 2-way valves of each analyzer is evacuated by a vacuum pump for about 1 min to quickly exchange the sample air in the main airflow line. During this evacuation process, a purge gas is introduced into the analyzers by using a 3-way valve (CKD, Co., Aichi, Japan, model AGD01V-T12-4R-FFF-1) to maintain a constant flow rate. The 3-way valve is useful in preventing a mixture of different gases when switching the purge gas off and starting the next flask analysis. The purge gas with a similar trace gas composition

as that of the ambient air is prepared in a 48 L aluminum high-pressure cylinder. This purge gas introduction enables us to avoid longer drifts of the analyzer signals associated with changes in the sample flow rate and cell pressure. Since we found that such drifts largely affect the analytical precision, the continuous air-supply system by switching from the sample or standard gas to the purge gas is essential for high-precision analyses of discrete flask samples in our trace gas measurement system.

2.4 Standard gases

Mole fraction measurements of all trace gases are traceable to five multicomponent working standard gases including CO_2 (365–430 ppm), CH_4 (1650–2050 ppb), CO (50–300 ppb) and N_2O (300–340 ppb) in purified natural air used as a balance gas. The isotopic compositions of the standard gases are different from those of ambient air, because the trace gases in the standards are obtained from burned petroleum or natural gases. The standards are filled in 48 L aluminum high-pressure cylinders, which are prepared using a volumetric method by a gas company (Japan Fine Products Corp., (JFP), Oyama, Japan). The drifts of the working standards are regularly investigated by comparing them with the JMA primary standard gases using a standard gas calibration system (e.g., Matsueda et al., 2004). In this JMA standard gas calibration system, CO_2 is analyzed by an NDIR (HORIBA Ltd., Kyoto, Japan, model VA510R), while other trace gases are analyzed by gas chromatographs (GCs) equipped with

a flame ionization detector (GC/FID: Shimadzu, Co., Ltd., Kyoto, Japan, model GC14B) for CH_4, a reduction gas detector (GC/HgO: RoundScience, Co., Ltd., Kyoto, Japan, model TRA-1) for CO, and an electron capture detector (GC/ECD: Shimadzu Co., Ltd., Kyoto, Japan, model GC-2014) for N_2O, respectively. Analytical precisions for repetitive measurements are less than 0.02 ppm for CO_2, 2 ppb for CH_4, 1 ppb for CO, and 0.3 ppb for N_2O.

All measured data in this paper are reported in parts per million (ppm = μmol mol^{-1}), and parts per billion (ppb = nmol mol^{-1}) by mole fraction in dry air traceable to the JMA primary standards in purified natural air used as a balance gas. Their standards are sent to the Central Calibration Laboratory (CCL) for calibration against the World Meteorological Organization (WMO) mole fraction scales for CO_2 (Zhao and Tans, 2006), CH_4 (Dlugokencky et al., 2005), CO (Novelli et al., 2003), and N_2O (Hall et al., 2007). The WMO mole fraction scales are propagated from the Global Monitoring Division (GMD) of the National Oceanic and Atmospheric Administration (NOAA) Earth System Research Laboratory, which serves as the CCL.

3 Results and discussions

3.1 Quality of flask air samples

Prior to the initiation of the analysis of flask samples at JMA, a quality-assurance test of the sample air passing through the air-conditioning system under actual flight conditions of the C-130H aircraft was made at a very low altitude of 1000 ft over MNM. This exercise was suitable around MNM, because the influence of the local sources and sinks on the MNM island is negligible on the trace gas observations there (Wada et al., 2007). At MNM, the Japan Meteorological Agency operates a ground-based monitoring station to conduct long-term atmospheric measurements of CO_2, CH_4, CO and O_3 as part of the Global Atmosphere Watch programme of the WMO (WMO/GAW).

During each low-level flight, 4 air samples were collected in stainless-steel flasks, because the titanium flasks coated with silicon, as well as the trace gas measurement system, at JMA were not ready at the time of the quality assurance test. Thus, the flask air samples collected were returned to the MRI for analysis of CO_2 by an NDIR, and CH_4 and CO by a GC/FID (Matsueda and Inoue, 1996; Matsueda et al., 1998). In total, 6 flights were made each month during July–December in 2010. All measurements at MRI were calculated based on the same WMO mole fraction scales to directly compare the data between the MRI and JMA.

Figure 2 shows the temporal variations of measured mole fractions for CO_2, CH_4 and CO obtained from the aircraft during the 6 experimental flights, and are compared to the hourly surface mean data (at 20 m height) obtained at the JMA monitoring station. Each aircraft value is an average of
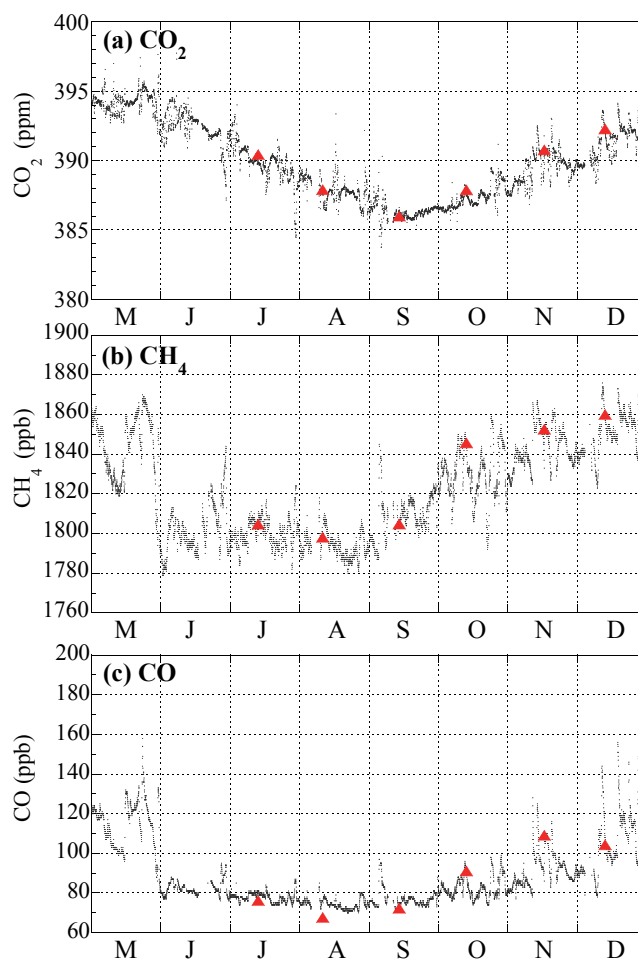

Fig. 2. Temporal variations of CO_2 **(a)**, CH_4 **(b)**, and CO **(c)** mole fractions over Minamitorishima during May–December in 2010. The red closed triangles and the solid dots represent aircraft measurements at 1000 ft (average of 4 flask samples) and hourly-averaged data from the ground-based station, respectively.

four flask measurements. The mean standard deviations (SD) of four measurements were ±0.09 ppm for CO_2, ±2.1 ppb for CH_4, and ±2.2 ppb for CO, due mainly to the overall flask sample analytical errors of less than ±0.1 ppm for CO_2, ±2 ppb for CH_4, and ±2 ppb for CO at MRI (Matsueda and Inoue, 1996; Matsueda et al., 1998; Matsueda et al., 2002). The averaged aircraft data show distinct seasonal variations, as well as short-term variations, that are quite similar to those from the surface hourly mean data (Fig. 2). To quantitatively compare between the aircraft and surface data, the difference between the two sets of measurements at the nearest sampling time were investigated instead of the hourly data. The mean differences of 24 individual measurements (aircraft data–surface data) were estimated to be +0.08 ppm with a SD of 0.23 ppm for CO_2, +0.24 ppb with a SD of 2.6 ppb for CH_4, and −0.17 ppb with a SD of 2.4 ppb for CO when 2 outlier data were omitted. These mean differences
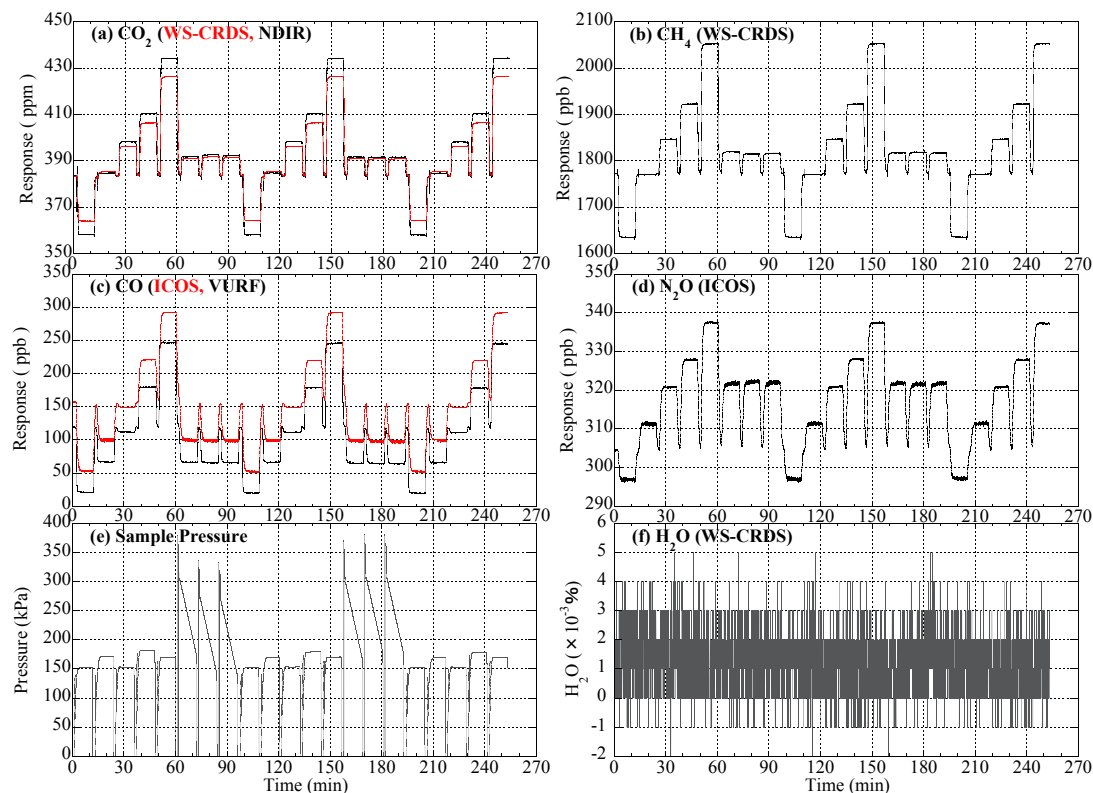
Fig. 3. An example of the response time series of CO_2 **(a)** for the NDIR and WS-CRDS analyzers, CH_4 **(b)** for the WS-CRDS analyzer, CO **(c)** for the VURF and ICOS analyzers, N_2O **(d)** for the ICOS analyzers, sample pressure **(e)** for the pressure sensor PS-7, and H_2O **(f)** for the WS-CRDS analyzer from the experimental analyses of 6 flask air samples together with 5 working standard gases. Details of the analytical sequence and procedure are described in the text.

are not viewed as significant, compared with the WMO-recommended limits (e.g., 0.1 ppm for CO_2, 2 ppb for CH_4 and 2 ppb for CO) (WMO, 2011), although the SDs are larger. The larger deviations might have been caused by several factors such as atmospheric variability, flask-to-flask variability, and possible flask sampling biases in the comparison between flask and in situ measurements, as pointed out by Karion et al. (2013). These results strongly suggest that CO_2, CH_4 and CO mole fractions in the sampled air are not significantly changed at least by passing it through the air-conditioning system of the C-130H aircraft. More experiments will be necessary for a precise evaluation of the reliability of the overall flask sampling procedure on board the C-130H aircraft by using the titanium flasks and the trace gas measurement system at JMA.

3.2 Storage test for sample flask

After sampling, it takes about 2–3 days for flasks to arrive at the JMA laboratory for mole fraction analysis. Therefore, to estimate the magnitude of the mole fraction drift of each trace gas in the flask during the transport, storage experiments using dry natural air were performed. Dry natural air obtained by passing through a dryer tube (3/4 inch in diameter, 35 cm

in length) packed with magnesium perchlorate was pumped into the flask to a pressure of 2–3 atm and was immediately analyzed for CO_2, CH_4 and CO mole fractions. After this initial analysis, the sample pressure decreased to less than 2 atm. The flasks were then kept at room temperature for 2–10 days, and were re-analyzed to calculate the drift. These analyses were performed using the NDIR and GC/FID measurement systems at MRI.

From the storage experiments, we estimated mean linear drifts of $+0.012\ \mathrm{ppm\,day^{-1}}$ with a standard deviation of $+0.017\ \mathrm{ppm\,day^{-1}}$ ($n = 48$) for CO_2, $+0.05\ \mathrm{ppb\,day^{-1}}$ with a SD of $0.27\ \mathrm{ppb\,day^{-1}}$ ($n = 28$) for CH_4, and $+0.19\ \mathrm{ppb\,day^{-1}}$ with a SD of $0.44\ \mathrm{ppb\,day^{-1}}$ ($n = 28$) for CO. Thus, all the trace gases increased in mole fraction, with a total increase over a 3 day storage period until analysis was about $+0.04 \pm 0.05$ ppm for CO_2, $+0.2 \pm 0.8$ ppb for CH_4, and $+0.6 \pm 1.3$ ppb for CO. These drifts were about twice as much as we had expected due to the fact that the sample pressure for the storage experiments was about 50 % lower than the pressure of the actual flask sampling using the C-130H aircraft. However, the significant scatter around the mean drift suggests that the flask-to-flask variability was quite large, and thus more experiments with longer time storage

Table 1. Results of repetitive measurements for CO_2, CH_4, CO and N_2O in a multicomponent standard gas filled into 6 flasks.

Trace gas	CO_2	CO_2	CH_4	CO	CO	N_2O
Analyzer	NDIR	WS-CRDS	WS-CRDS	VURF	ICOS	ICOS
Unit	(ppm)	(ppm)	(ppb)	(ppb)	(ppb)	(ppb)
Measured (A)*	387.16 (387.15)	387.23 (387.21)	1779.2 (1778.9)	101.7 (101.6)	101.6 (101.5)	313.98 (313.99)
SD	0.05 (0.04)	0.06 (0.04)	0.68 (0.31)	0.36 (0.33)	0.34 (0.26)	0.03 (0.03)
Assigned (B)**	387.17	387.17	1778.2	101.2	101.2	314.0
Difference (A)–(B)	−0.01 (−0.02)	0.06 (0.04)	0.99 (0.77)	0.49 (0.43)	0.43 (0.34)	−0.01 (−0.01)

* The measured value is an average of the 6 measurements ($n = 6$) from the measuring system developed in this study. The values in parentheses are an average of 5 measurements ($n = 5$) after excluding one flask whose measurements gave outliers. ** The assigned value is derived from the JMA standard gas calibration system using NDIR for CO_2 and gas chromatographs for CH_4, CO and N_2O.

will be necessary to precisely confirm the stability of the sample flasks. It has been reported that CO in a metal flask increases at a rate of about 0.6 ppb day^{-1} (e.g., Matsueda et al., 1998; Machida et al., 2008), but the silicon coating, as well as the precondition process, we carried out to prepare the flasks will help to minimize this problem.

3.3 Analysis and its precision

In the trace gas measurement system at JMA, 6 flask samples can be automatically analyzed together with the working standard gases. The data from the four analyzers, as well as from pressure and temperature sensors, are collected at an interval of 2 s. Figure 3 shows an example of the temporal variations of CO_2, CH_4, CO, N_2O, and H_2O as well sample pressure when 6 flasks with natural air and 5 standard gases are analyzed. To calibrate the measurements of the sample air, 5 working standard gases are introduced before and after 3 successive flask sample analyses. This frequency of the standard gas introduction is sufficient to precisely calibrate the sample measurements, because the instrumental drifts for all analyzers were found to be negligible within this time interval. Each analysis run for one flask sample or one standard gas takes about 12 min, consisting of 2 min for evacuation and sample purge of the airflow line, and the remaining 10 min for sample flow to the analyzers. For the 10 min sample flow, the air pressures of the flask samples decrease from about 300 kPa to 150 kPa (Fig. 3e), but no corresponding influences appear in all the output signal charts for CO_2, CH_4, CO, and N_2O, showing invariance of the analyzers with sample pressure (Fig. 3a–d). That is, when 1 min averaged analyzer signals are calculated, we find no significant fluctuations for the last 5 min of the 10 min sample flow. After the sample flow, the purge gas during the 2 min evacuation process is introduced into the analyzers and its corresponding peaks appear in all charts for CO_2, CH_4, CO, and N_2O (Fig. 3a–d). The water vapor (H_2O) signals from the

WS-CRDS analyzer show no significant difference between the sample air and dry standard gases with their H_2O content of less than 0.005 % (Fig. 3f). This result strongly suggests no significant influence of H_2O content on the analyses of the flask samples.

To evaluate the overall analytical precisions of the trace gas measurement system at JMA, one multicomponent standard gas with known mole fractions of the trace gases was filled into 6 sample flasks and then analyzed by the same analysis procedural sequence described above. Results from this experiment are summarized in Table 1. The 6 flask measurements from the WS-CRDS and ICOS analyzers showed high precisions for all the trace gas analyses with SDs of less than 0.06 ppm for CO_2, 0.68 ppb for CH_4, 0.36 ppb for CO, and 0.03 ppb for N_2O. When we calculate an average of 5 measurements after excluding one flask whose measurements gave outliers, the precisions (SDs) of the 5 measurements improved by about 10–20 % (Table 1). We have found that the estimated precisions were slightly influenced by a small inhomogeneity in the process of filling each of the 6 sample flasks with gas. It has been reported that the analytical precisions of the conventional methods used at the WMO Central Calibration Laboratory of NOAA/GMD are ~ 0.02 ppm for CO_2 by an NDIR (Zhao and Tans, 2006), ~ 1.2 ppb for CH_4 by a GC/FID (Dlugokencky et al., 2005), ~ 1–2 ppb for CO by a GC/HgO (Novelli et al., 2003), and ~ 0.12 ppb for N_2O by a GC/ECD (Hall et al., 2007). Compared with these high-precision methods, our analytical precisions using the laser-based instruments are better by about 2–4 times for CH_4, CO and N_2O, although the CO_2 data are slightly variable. In addition, Table 1 also shows that the measured mole fractions of all the trace gases agree with those assigned by the JMA standard gas calibration system to within the calibration errors, as stated in Sect. 2.4. When one flask whose measurements gave outliers was omitted, better agreements between the measured and assigned values were found for most of the trace gases (Table 1).

Table 2. Estimated isotope effects for CO_2, CH_4, CO and N_2O measured by two laser-based analyzers of WS-CRDS and ICOS.

	CO_2 (ppm)	CH_4 (ppb)	CO (ppb)	N_2O (ppb)
Isotope effect[a]	−0.14– −0.16	−0.05– −0.06	+0.001– +0.02	−0.03– −0.04
Range of mole fraction	360–420	1700–2200	30–500	310–340
Isotopic ratios of atmosphere[b]				
$\delta^{13}C$ (‰ VPDB)	−8	−47	−27	
$\delta^{18}O$ (‰ VSMOW)	+42		+10	+45
$\delta^{15}N$ (‰ VPDB)				+7
δD (‰ VSMOW)		−95		
Isotopic ratios of standard gas[c]				
$\delta^{13}C$ (‰ VPDB)	−33	−40	−25	
$\delta^{18}O$ (‰ VSMOW)	+13		+20	+26
$\delta^{15}N$ (‰ VPDB)				−2
δD (‰ VSMOW)		−175		

[a] Isotope effect is estimated when we use two laser-based instruments with a wavelength-scanned cavity ring-down spectroscopy (WS-CRDS) analyzer for CO_2 and CH_4 (Crosson, 2008), and an off-axis integrated cavity output spectroscopy (ICOS) analyzer for CO and N_2O (Baer et al., 2002).
[b] Isotopic ratios in the atmosphere are representative values from the measurements of atmospheric CO_2 (Nakazawa et al., 1993; Allison and Francey, 2007), CH_4 (Umezawa et al., 2009), CO (Kato et al., 1999), and N_2O (Ishijima et al., 2007).
[c] Isotopic ratios of CO_2 and CO in standard gases used in this study are the means obtained from the direct measurements by mass spectrometers (Tsunogai et al., 2002; Murayama et al., 2010). Isotopic ratios of standard gas for CH_4 are the representative values of fossil fuel CH_4 (Snover et al., 2000) similar to the measurements of other JFP standard gases by T. Umezawa (personal communication, 2011). Isotopic ratios of standard gas for N_2O are representative values derived from the measurements of other JFP standard gases by K. Ishijima (personal communication, 2011).

3.4 Calibration curve

Since the response linearity of the NDIR and VURF analyzers had been well examined (e.g., Gerbig et al., 1999; Zhao and Tans, 2006), we report here only the calibration curves for the new laser-based analyzers of the WS-CRDS and ICOS instruments. Figure 4 plots the raw signal versus the mole fraction for CO_2 and CH_4 from the WS-CRDS analyzer, and N_2O and CO from the ICOS analyzer. They are the analysis results of the five working standard gases. The mole fractions were determined by using the JMA standard gas calibration system based on the WMO mole fraction scales. It is noted that the CO mole fractions are given by using the VURF instrument in the trace gas measurement system with the JMA primary standard gases traceable to the WMO scale, because the GC/HgO method of the JMA standard gas calibration system has larger analytical errors due to the nonlinearity response of the HgO detector (Novelli et al., 2003).

As shown in Fig. 4, residuals between the linear fit curves and measured values are calculated to be less than 0.05 ppm for CO_2, less than 0.7 ppb for CH_4, less than 0.8 ppb for CO, and less than 0.3 ppb for N_2O. These deviations from the linear calibration curves are not significant considering the total analytical uncertainties associated with both the JMA standard gas calibration system and trace gas measurement system. These results indicate not only high linearity of the responses for both WS-CRDS and ICOS but also internal consistency of the assigned mole fractions for the 5 working

standard gases. The high linearity of CO by the same ICOS analyzer is also reported by Zellweger et al. (2012). Thus, we feel confident that the trace gas measurement system with the laser-based analyzers makes high-precision measurements that are accurately traceable to the WMO mole fraction scales.

3.5 Isotope effect and intercomparison

The laser-based analyzers of the WS-CRDS for CO_2 and CH_4 and of the ICOS for CO and N_2O potentially have some measurement errors due to their isotope effects (e.g., Chen et al., 2010). In our trace gas measurement system, the isotope effect results mainly from the differences in isotopic composition between a natural atmospheric sample and a working standard gas. Thus, we evaluated the isotope effects using a similar method reported by Chen et al. (2010) and the results are summarized in Table 2. All isotopic ratios in this study are expressed as delta (δ) values relative to the ratio of the reference materials of the Vienna Pee Dee Belemnite (VPDB) and Vienna Standard Mean Ocean Water (VSMOW).

To calculate the isotope effect of the WS-CRDS analysis for CO_2, we used −33 ‰ for $\delta^{13}C$ and +13 ‰ for $\delta^{18}O$ as CO_2 in our working standard gases. This isotopic composition was obtained from the direct measurements of our 5 working standard gases by using a mass spectrometer (Murayama et al., 2010). On the other hand, the $\delta^{13}C$ and $\delta^{18}O$ values of ambient CO_2 were assigned −8 ‰ (Nakazawa et
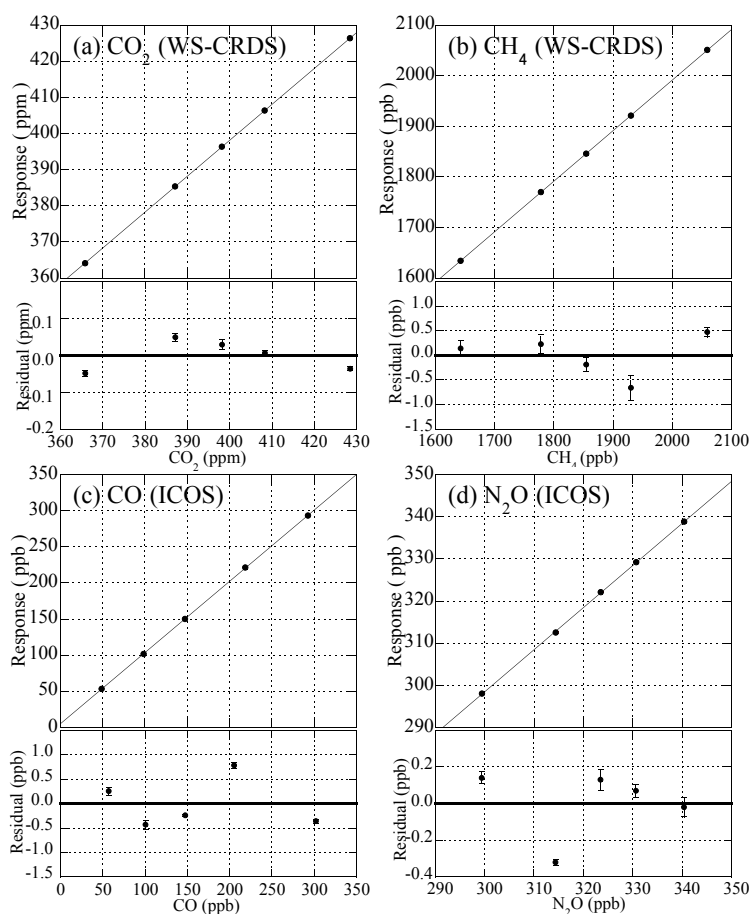
Fig. 4. Plots of the analyzer response versus assigned mole fractions of 5 working standard gases for CO_2 **(a)** and CH_4 **(b)** of the WS-CRDS analyzer, and CO **(c)** and N_2O **(d)** of the ICOS analyzer. The solid line represents a linear least squares fit to all the data points. Residuals of the fit are plotted in the lower panels.

al., 1993) and +42‰ (Allison and Francey, 2007), respectively. Using these values, the isotope effect was estimated to be about 0.14–0.16 ppm (CO_2 of 360–420 ppm), which is consistent with a previous estimate of 0.14–0.16 ppm (Chen et al., 2010; Tohjima et al., 2009).

Using the same method used for CO_2, we calculated the isotope effects associated with the WS-CRDS analyzer for CH_4 and with the ICOS analyzer for CO and N_2O (Table 2). The ICOS analyzer measures the number of $^{12}C^{16}O$ and $^{14}N_2^{16}O$ molecules (Baer et al., 2002), and determines the total CO and N_2O mole fractions by dividing the fractional abundance of $^{12}C^{16}O$ and $^{14}N_2^{16}O$ in ambient air by those in standard gas. Thus, the isotope effects of the ICOS can be calculated by the differences of fractional abundances between the standard gas and the ambient air. The isotope effects were estimated to be −0.05 to −0.06 ppb for CH_4, +0.001 to +0.02 ppb for CO, and −0.03 to −0.04 ppb for N_2O within the ambient air level. These values are one order of magnitude smaller than the analytical precisions of the WS-CRDS and ICOS analyzers, indicating no significant

isotope effects on the CH_4, CO, and N_2O measurements when our standard gases are used to calibrate the laser-based analyzers in our trace gas measurement system. In our estimation of CO, we measured directly the isotopic compositions in our working standard gases by using a continuous-flow isotope ratio mass spectrometry (Tsunogai et al., 2002). Although the direct measurements of isotopic ratios for CH_4 and N_2O are not available, the sensitivity tests strongly suggest that the isotope effects for CH_4 and N_2O are not significantly changed when we do calculations using a wider range of isotopic ratios in the standard gases.

Laser-based spectroscopic analyses are possibly biased not only by the isotope effect but also by the pressure-broadening effect resulting from the difference in the composition between a standard gas and ambient air. The pressure-broadening effect is caused mainly by the differences in the water vapor content and the composition of the matrix's gas (N_2, O_2, Ar) (Chen et al., 2010). The water vapor influence associated with the pressure-broadening and dilution effect is minimized by the drying procedure in our measuring system.
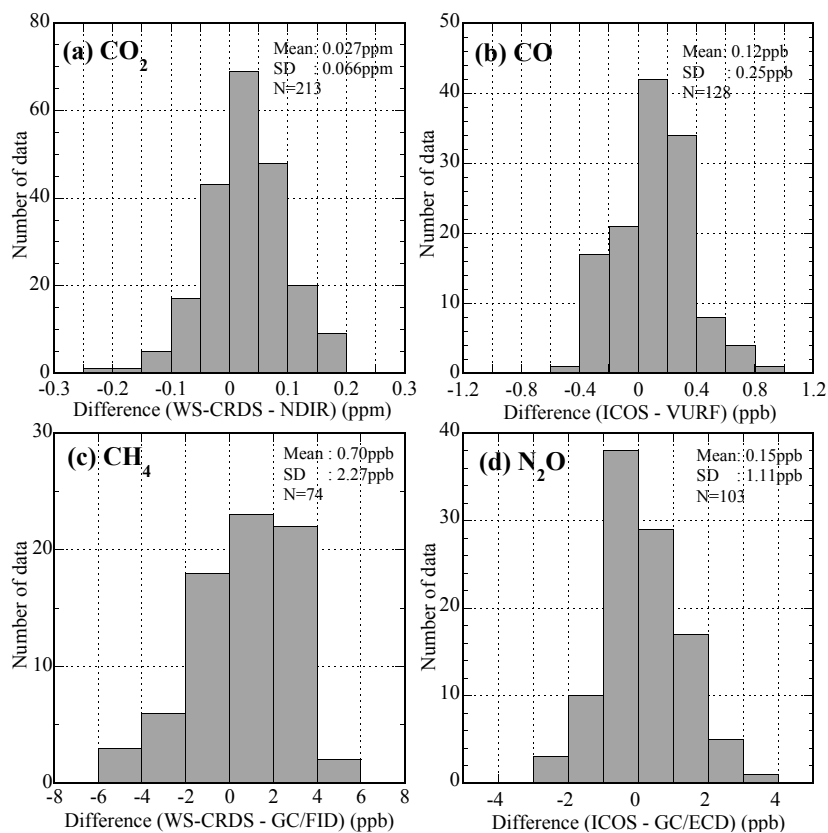
Fig. 5. Frequency distributions of the differences in air sample measurements for CO_2 between the WS-CRDS and the NDIR analyzers **(a)**, CO between the ICOS and the VURF analyzers **(b)**, CH_4 between the WS-CRDS and the GC/FID analyzers **(c)**, and N_2O between the ICOS and the GC/ECD analyzers **(d)**. The ranges of mole fractions in the air sample are 387–398 ppm for CO_2, 66–126 ppb for CO, 1796–1879 ppb for CH_4, and 320–327 ppb for N_2O.

The effect due to the matrix gas composition is also minimized by the use of purified natural air as the balance gas in our working standard gases, but a measurable influence due to a small difference in the matrix gas composition has been reported (Nara et al., 2012). Because it is difficult to quantify all of these individual effects, intercomparisons among different measuring techniques were made to evaluate the whole instrumental bias when we measure ambient air samples by using our working standard gases, as described below.

In our trace gas measurement system at JMA, the CO_2 mole fraction of our flask air samples is simultaneously measured by the WS-CRDS and NDIR analyzers, to compare their relative values. Both measurements are calibrated by the same 5 multicomponent working standard gases traceable to the WMO scales. Figure 5a shows a frequency distribution of the differences in the measured CO_2 mole fraction between the WS-CRDS and the NDIR analyzers for the flask air samples collected by the C-130H aircraft flights from February to August in 2011. The mean difference (WS-CRDS minus NDIR) was +0.03 ppm with a SD of 0.07 ppm when we compared 213 air sample analyses. We found no systematic difference as a function of CO_2 mole fraction within a

range from 387 to 398 ppm. The mean result shows a good agreement between the two different measuring techniques for CO_2 within the WMO-recommended limit (e.g., 0.1 ppm for CO_2) (WMO, 2011), although the standard deviations are larger than the mean bias due mainly to a combination of analytical errors from both the WS-CRDS and NDIR with about 0.8 ppm, as shown in Table 1.

The agreement of the averaged measurements between the WS-CRDS and the NDIR analyzers strongly suggests a similar level of isotope effect in the NDIR analyzer (caused by its optical band-pass filter) as observed in the WS-CRDS analyzer. Indeed, to experimentally evaluate the NDIR isotope effect, we measured the optical property of the filter by using a gravimetric $^{13}CO_2$-in-air mixture with CO_2 mole fraction of 380 ppm, following the method reported by Tohjima et al. (2009). The apparent mole fraction of the $^{13}CO_2$-in-air mixture determined by the NDIR analyzer used in this study was determined to be 16 ppm, indicating that its optical filter substantially reduced the response to $^{13}C^{16}O_2$. From this experimental result of the optical filter property, the isotope effect of our NDIR was theoretically calculated when we used -33‰ and -8‰ for $\delta^{13}C$ as CO_2 in our working standard

gases and ambient air, respectively. The NDIR isotope effect was 0.095–0.11 ppm (CO_2 of 360–420 ppm), which is similar to that of the WS-CRDS analyzer. This indicates that the isotope effects between the two analyzers are comparable to each other considering several uncertainties in the estimation.

We also performed an intercomparison of CO measured simultaneously by the ICOS and the VURF analyzers in the trace gas measurement system at JMA. Figure 5b shows a frequency distribution of the differences in the measured CO mole fraction between the VURF and the ICOS analyzers for 128 flask air samples collected by the C-130H aircraft flights from April to August in 2011. The mean difference (ICOS minus VURF) with a CO mole fraction range from 66 to 126 ppb was +0.12 ppb with a SD of 0.25 ppb, indicating the mean bias between the two analyzers is smaller than the WMO's interlaboratory compatibility goal (2 ppb) (WMO, 2011). This is consistent with the results of Zellweger et al. (2009) and Zellweger et al. (2012) who found, from their field intercomparison tests, an agreement between the ICOS, VURF and GC/HgO methods to within 1 %. That is, there does not appear to be any significant bias in the CO measuring technique using the ICOS analyzer, compared with the conventional GC/HgO and/or VURF methods commonly employed for background atmospheric CO observations (e.g., Novelli et al., 2003).

As for CH_4 and N_2O, only the WS-CRDS and ICOS laser-based analyzers are used in the trace gas measurement system. Thus, in order to assess the fidelity of these measurements, we carried out an intercomparison exercise in which flask air samples were analyzed by the GC/FID for CH_4 and GC/ECD for N_2O in the JMA standard gas calibration system after they were finished with the laser-based analyzers. In this intercomparison, the measured data from both the laser-based analyzers and the GC methods were calculated based on the same WMO mole fraction scales. The flask samples collected by the C-130H aircraft flights from February to August in 2011 were used for the comparison. Figure 5c and d show frequencies of the differences in CH_4 between the WS-CRDS and GC/FID analyzers, and in N_2O between the ICOS and GC/ECD analyzers, respectively. The mean difference for CH_4 (WS-CRDS minus GC/FID) was +0.70 ppb with a SD of 2.27 ppb ($n = 74$) for a mole fraction range from 1796 to 1879 ppb, while the mean difference for N_2O (ICOS minus GC/ECD) was +0.15 ppb with a SD of 1.11 ppb ($n = 103$) for a mole fraction range from 320 to 327 ppb. The mean biases are nearly the same or smaller than the WMO-recommended limits of 2 ppb for CH_4 and 0.1 ppb for N_2O, but the standard deviations are still relatively large compared to the mean values when several outliers with larger errors by the GC analyses were omitted. Karion et al. (2013) and Chen et al. (2013) reported that the difference between the continuous (CRDS) and flask (GC/FID) aircraft measurements for CH_4 showed a small bias of 0.4 ± 1.3 ppb during their field intercomparisons. Our results are consistent

with these previous studies showing that the bias in measuring CH_4 mole fraction by our WS-CRDS analyzer is smaller than the WMO's interlaboratory compatibility goal. On the other hand, there are no reports of a systematic validation of the bias of the N_2O measurements by the ICOS analyzer, although this analyzer is now available for field tests and in situ observations (Hammer et al., 2013; Zellweger et al., 2012). In the study, we have reported the results of our evaluation of the instrumental bias for N_2O measurement by the ICOS analyzer, although large uncertainties still remained. Further tests and analyses are needed since the ICOS analyzer has the potential to achieve high-precision measurements of atmospheric N_2O.

4 Conclusions

To set up a flask air sampling system by using a cargo C-130H aircraft, we examined its reliability for analyses of atmospheric trace gas mole fractions. The quality assurance test of the air-conditioning air used for the flask sampling was made by specially coordinated flights at a low altitude of 1000 ft over Minamitorishima. It was strongly suggested that the overall procedure of our flask sampling method in the aircraft is suitable to appropriately collect air samples without significant contamination and modification of the trace gas mole fractions. In addition, new flasks, with internal surfaces coated with silicon, were evaluated by the storage tests to ensure the stability of the trace gases. The average 2–3 day storage between the time of collection and analysis did not produce any large drift in the trace gas mole fractions, although the flask-to-flask variability still remained. To reduce this experimental uncertainty, we will be carrying out longer storage tests in the near future.

We also developed a trace gas measurement system for flask samples, comprising of Stirling coolers for sample drying, 5 working standard gases for calibration, and 4 analyzers to measure CO_2, CH_4, CO, and N_2O mole fractions. This system utilizes not only NDIR and VURF but also new laser-based analyzers using WS-CRDS and ICOS sensors. The laboratory experiment, using 6 flasks filled with a standard gas, showed high reproducibility of our laser-based analyses for all the trace gases. High linearity of the laser-based analyzers' response was confirmed using standard gases traceable to the WMO mole fraction scales. Their isotope effects were estimated to be negligible except for the CO_2 measurement. We demonstrated no significant biases in the averaged data from the aircraft sample measurements between the new laser-based spectroscopies and other different methods such as NDIR and GC. In this study, the laser-based instruments were employed first for discrete flask sample analyses to achieve high-precision measurements accurately traceable to the WMO mole fraction scales. At present, a sufficiently large amount of sample air (about 3.4 L) is conservatively used at the first application step, but the trace gas

measurement system and the analytical condition could be improved to utilize a smaller amount of sample air. For this improvement, further experiments will be necessary to examine the appropriate analytical conditions under which we can lower the flow rate but still maintain sufficiently fast response times, by perhaps using a compact measurement system. Thus, our measurement system has the potential to be widely used for flask sample analyses based on the laser-based instruments, although more precise evaluation of the instrumental biases will be needed.

Using the C-130H military aircraft, JMA continues to carry out the flask sampling program for trace gas measurements once a month as a long-term operational monitoring program. Thus, the JMA's aircraft observations could provide a useful dataset of sufficiently high quality over the western North Pacific to better understand the trace gas emissions in East Asia and their long-range transports through the free troposphere. The dataset is posted on the WMO's World Data Centre for Greenhouse Gases (WMO/WGCGG, http://ds.data.jma.go.jp/gmd/wdcgg/wdcgg.html) operated by JMA in Tokyo.

Edited by: A. C. Manning

References

Akimoto, H.: Global air quality and pollution, Science, 302, 1716–1719, doi:10.1126/science.1092666, 2003.

Allison, C. E. and Francey, R. J.: Verifying Southern Hemisphere trends in atmospheric carbon dioxide stable isotopes, J. Geophys. Res., 112, D21304, doi:10.1029/2006JD007345, 2007.

Baer, D. S., Paul, J. B., Gupta, M., and O'Keefe, A.: Sensitive absorption measurements in the near-infrared region using off-axis integrated-cavity-output spectroscopy, Appl. Phys. B, 75, 261–265, doi:10.1007/s00340-002-0971-z, 2002.

Bergamaschi, P., Frankenberg, C., Meirink, J. F., Krol, M., Villani, M. G., Houweling, S., Dentener, F., Dlugokencky, E. J., Miller, J. B., Gatti, L. V., Engel, A., and Levin, I.: Inverse modelling of global and regional CH$_4$ emissions using SCIAMACHY satellite retrievals, J. Geophys. Res., 114, D22301, doi:10.1029/2009JD012287, 2009.

Brenninkmeijer, C. A. M., Crutzen, P., Boumard, F., Dauer, T., Dix, B., Ebinghaus, R., Filippi, D., Fischer, H., Franke, H., Frieß, U., Heintzenberg, J., Helleis, F., Hermann, M., Kock, H. H., Koeppel, C., Lelieveld, J., Leuenberger, M., Martinsson, B. G., Miemczyk, S., Moret, H. P., Nguyen, H. N., Nyfeler, P., Oram, D., O'Sullivan, D., Penkett, S., Platt, U., Pupek, M., Ramonet, M., Randa, B., Reichelt, M., Rhee, T. S., Rohwer, J., Rosenfeld, K., Scharffe, D., Schlager, H., Schumann, U., Slemr, F., Sprung, D., Stock, P., Thaler, R., Valentino, F., van Velthoven, P., Waibel, A., Wandel, A., Waschitschek, K., Wiedensohler, A., Xueref-Remy, I., Zahn, A., Zech, U., and Ziereis, H.: Civil Aircraft for the regular investigation of the atmosphere based on an instrumented container: The new CARIBIC system, Atmos. Chem. Phys., 7, 4953–4976, doi:10.5194/acp-7-4953-2007, 2007.

Chen, H., Winderlich, J., Gerbig, C., Hoefer, A., Rella, C. W., Crosson, E. R., Van Pelt, A. D., Steinbach, J., Kolle, O., Beck, V., Daube, B. C., Gottlieb, E. W., Chow, V. Y., Santoni, G. W., and Wofsy, S. C.: High-accuracy continuous airborne measurements of greenhouse gases (CO$_2$ and CH$_4$) using the cavity ring-down spectroscopy (CRDS) technique, Atmos. Meas. Tech., 3, 375–386, doi:10.5194/amt-3-375-2010, 2010.

Chen, H., Karion, A., Rella, C. W., Winderlich, J., Gerbig, C., Filges, A., Newberger, T., Sweeney, C., and Tans, P. P.: Accurate measurements of carbon monoxide in humid air using the cavity ring-down spectroscopy (CRDS) technique, Atmos. Meas. Tech., 6, 1031–1040, doi:10.5194/amt-6-1031-2013, 2013.

Crosson, E. R.: A cavity ring-down analyzer for measuring atmospheric levels of methane, carbon dioxide, and water vapor, Appl. Phys. B-Lasers O., 92, 403–408, doi:10.1007/s00340-008-3135-y, 2008.

Dlugokencky, E. J., Myers, R. C., Lang, P. M., Masarie, K. A., Crotwell, A. M., Thoning, K. W., Hall, B. D., Elkins, J. W., and Steele, L. P.: Conversion of NOAA atmospheric dry air CH$_4$ mole fractions to a gravimetrically prepared standard scale, J. Geophys. Res., 110, D18306, doi:10.1029/2005JD006035, 2005.

Gerbig, C., Smitgen, S., Kley, D., Volz-Thomas, A., Dewey, K., and Haaks, D.: An improved fast-response vacuum-UV resonance fluorescence CO instrument, J. Geophys. Res., 104, 1699–1704, doi:10.1029/1998JD100031, 1999.

Gregg, J. S., Andres, R. J., and Marland, G.: China: Emissions pattern of the world leader in CO$_2$ emissions from fossil consumption and cement production, Geophs. Res. Lett., 35, L08806, doi:10.1029/2007GL032887, 2008.

Hall, B. D., Dutton, G. S., and J. W. Elkins, J. W.: The NOAA nitrous oxide standard scale for atmospheric observations, J. Geophys., Res., 112, D09305, doi:10.1029/2006JD007954, 2007.

Hammer, S., Konrad, G., Vermeulen, A. T., Laurent, O., Delmotte, M., Jordan, A., Hazan, L., Conil, S., and Levin, I.: Feasibility study of using a "travelling" CO$_2$ and CH$_4$ instrument to validate continuous in situ measurement stations, Atmos. Meas. Tech., 6, 1201–1216, doi:10.5194/amt-6-1201-2013, 2013.

Huang, J., Golombek, A., Prinn, R., Weiss, R., Fraser, P., Simmonds, P., Dlugokencky, E. J., Hall, B., Elkins, J., Steele, P., Langenfelds, R., Krummel, P., Dutton, G., and Porter, L.: Estimation of regional emissions of nitrous oxide from 1997 to

2005 using multinetwork measurements, a chemical transport model, and an inverse method, J. Geophys., Res., 113, D17313, doi:10.1029/2007JD009381, 2008.

Ishijima, K., Sugawara, S. Kawamura, K., Hashida, G., Morimoto, S., Murayama, S., Aoki, S., and Nakazawa, T.: Temporal variations of the atmospheric nitrous oxide concentration and its $\delta^{15}N$ and $\delta^{18}O$ for the latter half of the 20th century reconstructed from firn air analyses, J. Geophys. Res., 112, D03305, doi:10.1029/2006JD007208, 2007.

Jacob, D. J., Crawford, J. H., Kleb, M. M., Connors, V. S., Bendura, R. J., Raper, J. L., Sachse, G. W., Gille, J. C., Emmons, L., and Heald, C. L.: Transport and chemical evolution over the Pacific (TRACE-P) aircraft mission: Design, execution, and first results, J. Geophys. Res., 108, 9000, doi:10.1029/2002JD003276, 2003.

Karion, A., Sweeney, C., Tans, P., and Newberger, T.: AirCore: An Innovative atmospheric sampling system, J. Atmos. Ocean. Tech., 27, 1839–1853, doi:10.1175/2010JTECHA1448.1, 2010.

Karion, A., Sweeney, C., Wolter, S., Newberger, T., Chen, H., Andrews, A., Kofler, J., Neff, D., and Tans, P.: Long-term greenhouse gas measurements from aircraft, Atmos. Meas. Tech., 6, 511–526, doi:10.5194/amt-6-511-2013, 2013.

Kato, S., Akimoto, H., Bräunlich, M., Röckmann, T., and C. A. M. Brenninkmeijer, C. A. M.: Measurements of stable carbon and oxygen isotopic compositions of CO in automobile exhausts and ambient air from semi-urban Mainz, Germany, Geochem. J., 33, 73–77, 1999.

Liang, Q., Jaeglé, L., Jaffe, D. A., Weiss-Penzias, P., Heckman, A. and Snow, J. A.: Long-range transport of Asian pollution to the northeast Pacific: Seasonal variations and transport pathways of carbon monoxide, J. Geophys., Res., 109, D23S07, doi:10.1029/2003JD004402, 2004.

Machida, T., Kita, K., Kondo, Y., Blake, D., Kawakami, S., Inoue, G., and Ogawa, T.: Vertical and meridional distributions of the atmospheric CO_2 mixing ratio between northern midlatitudes and southern subtropics, J. Geophys. Res., 108, 8401, doi:10.1029/2001JD000910, 2003.

Machida, T., Matsueda, H., Sawa, Y., Nakagawa, Y., Hirotani, K., Kondo, N., Goto, K., Nakazawa, T., Ishikawa, K., and Ogawa, T.: Worldwide measurements of atmospheric CO_2 and other trace gas species using commercial airlines, J. Atmos. Ocean. Tech., 25, 1744–1754, doi:10.1175/2008JTECHA1082.1, 2008.

Marenco, A., Thouret, V., Nédélec, P., Smit, H., Helten, M., Kley, D., Karcher, F., Simon, P., Law, K., Pyle, J., Poschmann, G., Von Wrede, R., Hume, C., and Cook, T.: Measurement of ozone and water vapor by Airbus in-service aircraft: The MOZAIC airborne program, An overview, J. Geophys. Res., 103, 25631–25642, doi:10.1029/98JD00977, 1998.

Matsueda, H. and Inoue, H. Y.: Measurements of atmospheric CO_2 and CH_4 using a commercial airliner from 1993 to 1994, Atmos. Environ., 30, 1647–1655, doi:10.1016/1352-2310(95)00374-6, 1996.

Matsueda, H., Inoue, H. Y., Sawa, Y., Tsutsumi, Y., and Ishii, M.: Carbon monoxide in the upper troposphere over the western Pacific between 1993 and 1996, J. Geophys. Res., 103, 19093–19110, doi:10.1029/98JD01598, 1998.

Matsueda, H., Inoue, H. Y., and Ishii, M.: Aircraft observation of carbon dioxide at 8–13 km altitude over the western Pacific from 1993 to 1999, Tellus, 54B, 1–21, doi:10.1034/j.1600-0889.2002.00304.x, 2002.

Matsueda, H., Sawa, Y., Wada, A., Inoue, H. Y., Suda, K., Hirano, Y., Tsuboi, K., and Nishioka, S.: Methane standard gases for atmospheric measurements at the MRI and JMA and intercomparison experiments, Pap. Meteorol. Geophys., 54, 91–109, doi:10.2467/mripapers.54.91, 2004.

Murayama, S., Harada, K., Gotoh, K., Kitao, T., Watai, T., and Yamamoto, S.: On large variations in atmospheric CO_2 concentration observed over the central and western Pacific Ocean, J. Geophys. Res., 108, 4243, doi:10.1029/2002JD002729, 2003.

Murayama, S., Takamura, C., Yamamoto, S., Saigusa, N., Morimoto, S., Kondo, H., Nakazawa, T., Aoki, S., Usami, T., and Kondo, M.: Seasonal variations of atmospheric CO_2, $\delta^{13}C$, and $\delta^{18}O$ at a cool temperate deciduous forest in Japan: Influence of Asian monsoon, J. Geophys. Res., 115, D17304, doi:10.1029/2009JD013626, 2010.

Nakazawa, T., Morimoto, S., Aoki, S., and Tanaka, M.: Time and space variations of the carbon isotopic ratio of tropospheric carbon dioxide over Japan, Tellus, 45B, 258–274, doi:10.1034/j.1600-0889.1993.t01-2-00004.x, 1993.

Nara, H., Tanimoto, H., Tohjima, Y., Mukai, H., Nojiri, Y., Katsumata, K., and Rella, C. W.: Effect of air composition (N_2, O_2, Ar, and H_2O) on CO_2 and CH_4 measurement by wavelength-scanned cavity ring-down spectroscopy: calibration and measurement strategy, Atmos. Meas. Tech., 5, 2689–2701, doi:10.5194/amt-5-2689-2012, 2012.

Niwa, Y., Machida, T., Sawa, Y., Matsueda, H., Schuck, T. J., Brenninkmeijer, C. A. M., Imasu, R., and Satoh, M.: Imposing strong constraints on tropical terrestrial CO_2 fluxes using passenger aircraft based measurements, J. Geophys. Res., 117, D11303, doi:10.1029/2012JD017474, 2012.

Novelli, P. C., Masarie, K. A., Lang, P. M., Hall, B. D., Myers, R. C., and Elkins, J. W.: Reanalysis of tropospheric CO trends: Effects of the 1997–1998 wildfires, J. Geophys. Res., 108, 4464, doi:10.1029/2002JD003031, 2003.

Richardson, S. J., Miles, N. L., Davis, K. J., Crosson, E. R., Rella, C. W., and Andrews, A. E.: Field testing of cavity ring-down spectroscopy analyzers measuring carbon dioxide and water vapor, J. Atmos. Ocean. Tech., 29, 397–406, doi:10.1175/JTECH-D-11-00063.1, 2012.

Sawa, Y., Matsueda, H., Makino, Y., Inoue, H. Y., Murayama, S., Hirota, M., Tsutsumi, Y., Zaizen, Y., Ikegami, M., and Okada, K.: Aircraft observation of CO_2, CO, O_3 and H_2 over the North Pacific during PACE-7 campaign, Tellus, 56B, 2–20, doi:10.1111/j.1600-0889.2004.00088.x, 2004.

Sawa, Y., Tanimoto, H., Yonemura, S., Matsueda, M., Mukai, H., Wada, A., Taguchi, S., Hayasaka, T., Tsuruta, H., Tohjima, Y., Mukai, H., Kikuchi, N., Katagiri, S., and Tsuboi, K.: Carbon monoxide for widespread pollution events observed over the western North Pacific during EAREX campaign 2005, J. Geophys. Res., 112, D22S26, doi:10.1029/2006JD008055, 2007.

Sawa, Y., Machida, T., and Matsueda, H.: Aircraft observations of the seasonal variation in the transport of CO_2 in the upper atmosphere, J. Geophys. Res., 117, D05305, doi:10.1029/2011JD016933, 2012.

Schuck, T. J., Brenninkmeijer, C. A. M., Slemr, F., Xueref-Remy, I., and Zahn, A.: Greenhouse gas analysis of air samples collected onboard the CARIBIC passenger aircraft, Atmos. Meas. Tech., 2, 449–464, doi:10.5194/amt-2-449-2009, 2009.

Smith, A. D., Barone, G. A., Higgins, M. E., Kendall, B. R. F., and Lavrich, D. J.: Method for chemical vapor deposition of silicon on to substrates for use in corrosive and vacuum environments, United States Patent No.7, 070, 833B2, 2006.

Snover, A. K., Quay, P. D., and Hao, W. M.: The D/H content methane emitted from biomass burning, Global Biogeochem. Cy., 14, 11–24, doi:10.1029/1999GB900075, 2000.

Stephens, B. B., Gurney, K. R., Tans, P. P., Sweeney, C., Peters, W., Bruhwiler, L. M., Ciais, P., Ramonet, M., Bousquet, P., Nakazawa, T., Aoki, S., Machida, T., Inoue, G., Vinnichenko, N., Lloyd, J., Jordan, A., Heimann, M., Shibistova, O. B., Langenfelds, R. L., Steele, L. P., Francey, R. J., and Denning, A. S.: Weak northern and strong tropical land carbon uptake from vertical profiles of atmospheric CO_2, Science, 316, 1732–1735, doi:10.1126/science.1137004, 2007.

Stephens, B. B., Miles, N. L., Richardson, S. J., Watt, A. S., and Davis, K. J.: Atmospheric CO_2 monitoring with single-cell NDIR-based analyzers, Atmos. Meas. Tech., 4, 2737–2748, doi:10.5194/amt-4-2737-2011, 2011.

Terao, Y., Mukai, H., Nojiri, Y., Machida, T., Tohjima, Y., Saeki, T., and Maksyutov, S.: Interannual variability and trends in atmospheric methane over the western Pacific from 1994 to 2010, J. Geophys. Res., 116, D14303, doi:10.1029/2010JD015467, 2011.

Tohjima, Y., Machida, T., Utiyama, M., Katsumata, M., Fujimura, Y., and Maksyutov, S.: Analysis and presentation of in situ atmospheric methane measurements from Cape Ochiishi and Hateruma Island, J. Geophys. Res., 107, 4148, doi:10.1029/2001JD001003, 2002.

Tohjima, Y., Katsumata, K., Morino, I., Mukai, H., Machida, T., Akama, I., Amari, T., and Tsunogai, U.: Theoretical and experimental evaluation of the isotope effect of NDIR analyzer on atmospheric CO_2 measurement, J. Geophys. Res., 114, D13302, doi:10.1029/2009JD011734, 2009.

Tsunogai, U., Nakagawa, F., Komatsu, D. D., and Gamo, T.: Stable carbon and oxygen isotopic analysis of atmospheric carbon monoxide using continuous-flow isotope ratio MS by isotope ratio monitoring of CO, Anal. Chem., 74, 5695–5700, doi:10.1021/ac020290x, 2002.

Umezawa, T., Aoki, S., Nakazawa, T., and Morimoto, S.: A high-precision measurement system for carbon and hydrogen isotopic ratios of atmospheric methane and its application to air samples collected in the western Pacific region, J. Meteor. Soc. Jpn., 87, 365–379, doi:10.2151/jmsj.87.365, 2009.

Wada, A., Sawa, Y., Matsueda, H., Taguchi, S., Murayama, S., Okubo, S., and Tsutsumi, Y.: Influence of continental air mass transport on atmospheric CO_2 in the western North Pacific, J. Geophys. Res., 112, D07311, doi:10.1029/2006JD007552, 2007.

Wada, A., Matsueda, H., Sawa, Y., Tsuboi, K., and Okubo, S.: Seasonal variation of enhancement ratios of trace gases observed over 10 years in the western North Pacific, Atmos. Environ, 45, 2129–2137, doi:10.1016/j.atmosenv.2011.01.043, 2011.

Winderlich, J., Chen, H., Gerbig, C., Seifert, T., Kolle, O., Lavriš, J. V., Kaiser, C., Höfer, A., and Heimann, M.: Continuous low-maintenance $CO_2/CH_4/H_2O$ measurements at the Zotino Tall Tower Observatory (ZOTTO) in Central Siberia, Atmos. Meas. Tech., 3, 1113–1128, doi:10.5194/amt-3-1113-2010, 2010.

WMO: 15th WMO/IAEA Meeting of Exerts on Carbon Dioxide, Other Greenhouse Gases and Related Tracers Measurement Techniques, GAW Report, No. 194, 2011.

Yashiro, H., Sugawara, S., Sudo, K., Aoki, S., and Nakazawa, T.: Temporal and spatial variations of carbon monoxide over the western part of the Pacific Ocean, J. Geophys. Res., 114, D08305, doi:10.1029/2008JD010876, 2009.

Zellweger, C., Hüglin, C., Klausen, J., Steinbacher, M., Vollmer, M., and Buchmann, B.: Inter-comparison of four different carbon monoxide measurement techniques and evaluation of the long-term carbon monoxide time series of Jungfraujoch, Atmos. Chem. Phys., 9, 3491–3503, doi:10.5194/acp-9-3491-2009, 2009.

Zellweger, C., Steinbacher, M., and Buchmann, B.: Evaluation of new laser spectrometer techniques for in-situ carbon monoxide measurements, Atmos. Meas. Tech., 5, 2555–2567, doi:10.5194/amt-5-2555-2012, 2012.

Zhao, C. L. and Tans, P. P.: Estimating uncertainty of the WMO mole fraction scale for carbon dioxide in air, J. Geophys. Res., 111, D08S09, doi:10.1029/2005JD006003, 2006.